Dental Materials Journal 2023; 42(2): 177–186

A statistical model of the rate-dependent fracture behavior of dental polymer-based biomaterials

Peer SCHRADER[1], Alexander SCHMIDT[2], Maximiliane A. SCHLENZ[2], Stefan KOLLING[1], Bernd WÖSTMANN[2] and Marcel BERLINGER[1]

[1] *Institute of Mechanics and Materials, Technische Hochschule Mittelhessen, Wiesenstrasse 14, 35390 Giessen, Germany*
[2] *Department of Prosthodontics, Dental Clinic, Justus Liebig University Giessen, Schlangenzahl 14, 35392 Giessen, Germany*
Corresponding author, Alexander SCHMIDT; E-mail: alexander.schmidt@dentist.med.uni-giessen.de

An insight into the fracture behavior of dental polymer-based biomaterials is important to reduce safety hazards for patients. The crack-driven fracture process of polymers is largely stochastic and often dependent on the loading rate. Therefore, in this study, a statistical model was developed based on three-point bending tests on dental polymethyl methacrylate at different loading rates. The fracture strains were investigated (two-parameter Weibull distribution (2PW)) and the rate-dependency of the 2PW parameters were examined (Cramér-von Mises test (CvM)), arriving at the conclusion that there could be a limiting distribution for both quasi-static and dynamic failure. Based on these findings, a phenomenological model based on exponential functions was developed, which would further facilitate the determination of the failure probability of the material at a certain strain with a given strain rate. The model can be integrated into finite element solvers to consider the stochastic fracture behavior in simulations.

Keywords: Biocompatible materials, Weibull statistics, Dental materials, Fracture strain, Statistical models

INTRODUCTION

Polymethyl methacrylate (PMMA) is an important material in medicine, especially dentistry, and is used in several applications because of its compatibility with human tissue, reliability, processing features, and low toxicity[1)]. However, when applied in the context of dental applications, the fracture behavior of PMMA is difficult to predict. The failure of a PMMA component in medical use will result in additional visits to the doctor, increased treatment costs, and symptoms such as, pain, aspiration risk, or similar health hazards for the patient. The aim of this study is to create a statistical model that allows the determination of a component's fracture probability given the applied strain and strain rate, contributing to the statistical prediction of the fracture behavior of PMMA and, hence, ensuring patient safety in the design of medical supplies. The statistical model presented in this study can be integrated into finite element simulations, allowing both stochastic finite element simulations and designing medical restorations with specific statistical safety targets.

For example, PMMA is used as a bone cement, for screw fixation in the bone, as a filler for bone cavities and skull defects, and vertebral stabilization in osteoporotic patients[1-5)]. PMMA is also used in and close to the human eye, such as in interocular lenses, rigid contact lenses, or eyeglass lenses[1,6)]. Most importantly, PMMA is widely used in dental applications[7-11)]. It is important to recognize that in all the aforementioned uses of PMMA (and similar amorphous thermoplastics such as polyethene, polypropylene, and polyether ether ketone), it is essential to possess good knowledge of the fracture behavior of the used components, as the fracture of a polymer-based component *in vivo* may have serious consequences for the health and safety of the patient and further will, in any case, require de novo medical treatment.

In dentistry, a common problem with restorations that are fabricated using PMMA are fractures in the application of fixed or removable dental prostheses (crowns, bridges, and partial or complete dentures)[12,13)]. Studies on this topic have mostly focused on permanent dental materials (*e.g.* fixed partial dentures made of metal alloy or ceramics), so far, lacking data on the fracture behavior of semi-permanent materials (*e.g.* fixed and removable interim dentures made of PMMA). A precise prediction of fracture behavior is very difficult because many parameters, such as material properties, force peaks, chewing force, and chewing velocity, must be taken into account[14)]. On the one hand, the failure risks of the respective materials are inherent in their properties. On the other hand, each patient has different boundary conditions for a dental biomaterial, ranging from different chewing velocities to varying chewing forces from patient to patient. Furthermore, load cases can range from low forces up to patients with bruxism, where chewing force peaks can occur, or in the extreme case, when masticating very hard food components, (*e.g.*, cherry pit) all at once[15)]. Possible consequences of denture fractures include discomfort, pain, and the occurrence of caries up to the possible loss of teeth. More dramatically, there is a risk of swallowing or aspiration of fragments, especially in cases of fractures during sleep[16)]. In addition to the possible risks for the patient, the costs for new production, the costs within the dental practice, and the associated time and economic consequences must be mentioned. Even though the use of semi-permanent restorations is limited to a maximum of one year, new fabrication requires additional time and costs, as well as

Received Jul 19, 2022: Accepted Sep 13, 2022
doi:10.4012/dmj.2022-163 JOI JST.JSTAGE/dmj/2022-163

an additional burden for the patients.

Therefore, it would be preferable to statistically approximate the probability of failure for different polymer-based biomaterials based on experimentally obtained material properties. Hence, the aim of the present study is to make a statement about a component failure risk based on three-point bending tests (3PBT). The tests are conducted on polymer-based biomaterials to ultimately increase patient safety and comfort by predicting the failure probability of restorations in consideration of rate-dependent material behavior. An implementation of finite element models, such as the simulation of dental prostheses by Schrader *et al.*[17] is deemed worthwhile. It should be noted in advance that although we focused on dental PMMA in this study, the methodology developed in this study is considered usable for all kinds of above-mentioned dental biomaterials and other thermoplastics.

To serve this purpose, we advocate using Weibull statistics, as this is commonly used in the field of dental biomaterial science. For example, in the literature, the Weibull distribution has been used to describe the fatigue behavior of dental biomaterials[18,19] and to compare the impact of surface treatments on a material's fracture behavior or to report the strength of dental materials in general[20-22]. It is important to note that the aforementioned studies using Weibull statistics in dental materials science investigated the stresses at fracture. Although this seems sufficient for ceramics or other linear elastic materials, this approach is only reasonable for PMMA if fracture mirrors can be found and the stress in fracture could be approximated[23]. As PMMA shows stress relaxation to a significant extent[24], the determination of failure stresses from experiments is problematic. Although the rate-dependency of the material behavior of PMMA has been investigated in an increasing number of studies in mechanical engineering (see Refs. 2, 25–29 for example), it has so far been mostly neglected in dental biomaterials science. Only recently, new studies have been investigating the influence of the rate-dependency on the behavior of provisional treatments consisting of PMMA, with the conclusion that the rate-dependency of PMMA must not be neglected because the fracture behavior of a provisional treatment consisting of PMMA is heavily impacted by the loading velocity[17,24,30]. As thermoplastics generally behave in this manner, it is likely that the same also applies to many other polymer-based materials or hybrid materials with a thermoplastic matrix, used in the medical field.

Hence, this study proposes a new approach to determine the failure risk of polymer-based components by considering the fracture strain and strain rate from 3PBT. Here, we rely on the results obtained by Schmidt *et al.*[24], who performed a large variety of 3PBT at different loading velocities. From this, we derive a methodology that can be used to model the failure risk of a component under different boundary conditions of the applied strain and strain rate.

We begin by summarizing the most important findings of subsequent studies on the rate-dependency of the tested material. Furthermore, we shall present the necessary theoretical background of the statistical procedure, including a brief overview of the two-parameter Weibull (2PW) distribution, probability and parameter estimation, and the goodness of fit criterion. From these, the cumulative distribution functions (CDFs) at each tested strain rate were determined and tested for goodness of fit. To investigate the rate-dependency of the material fracture behavior, we would also present the Cramèr-von Mises test (CvM), which is used to investigate whether two samples of fracture strains obtained at different strain rates, would come from the same unknown continuous distribution. We shall also include remarks on the coefficient of determination, which is used to estimate the goodness of our proposed model. The central finding of the presented procedure is a model from which the fracture probability of the tested material can be determined for a given strain and strain rate. Eventually, we present the clinical application of our methodology and its clinical benefits as well as possible further applications.

MATERIALS AND METHODS

Investigated data

To statistically investigate the fracture behavior of a material under different clinically relevant loading rates, a large experimental database is necessary. Therefore, we referred to the results obtained by Schmidt *et al.*[24] who had generated a large database for commercial dental PMMA using 3PBT. Their 3PBT results were examined for the fracture behavior of the tested material. Schmidt *et al.* had investigated the behavior of specimens consisting of Telio CAD (Ivoclar-Vivadent, Schaan, Lichtenstein; cross-linked PMMA, percentage by weight of 99.5%, pigments <1%, no further fillers[7,9,10]) at different loading velocities, under laboratory conditions. The specimens used were sawed from Telio CAD blocks water-cooled with a high-precision saw (IsoMet 1000, Buehler, Esslingen, Germany), achieving specimen dimensions of 2×2×40 mm and 2×2×55 mm. In their study, it was found that elastic modulus and fracture strain were dependent on the initial strain rate $\dot{\varepsilon}$ during 3PBT. In Table 1, the tested rates, specimen geometries, and measurement systems that were used are provided as an overview. For a better overview, the strain rates tested by Schmidt *et al.*[24] are referred to as $\dot{\varepsilon}_1$, …, $\dot{\varepsilon}_6$.

Furthermore, it was found that the fracture strain could be calculated from the linear elastic beam theory even during a quasistatic 3PBT, whereas the fracture stress could not, as stress relaxation was observed to a significant extent[24].

Statistical procedure

1. Two-parameter Weibull distribution and parameter estimation

For ceramics and mineral glasses, the fracture probability is typically described by 2PW. For PMMA, it was also found to provide a good reproduction of the experimental data, as shown in the stochastic analyses

Table 1 Strain rates tested by Schmidt *et al.*[24]

Ref.	Crosshead velocity	Strain rate (1/s)	Sample size (–)	Testing machine and specimen geometry
$\dot{\varepsilon}_1$	1 mm/min	6.920×10^{-4}	20	Servo-electric universal test machine Inspect 5 (Hegewald & Peschke, Nossen, Germany), 2×2×40 mm specimens, support distance of 17 mm
$\dot{\varepsilon}_2$	10 mm/min	6.920×10^{-3}	20	
$\dot{\varepsilon}_3$	100 mm/min	6.920×10^{-2}	20	
$\dot{\varepsilon}_4$	0.5 m/s	4.898	10	Impetus Pendulum System (4a technology, Traboch, Austria), 2×2×55 mm specimens, support distance of 35 mm
$\dot{\varepsilon}_5$	1.0 m/s	9.796	10	
$\dot{\varepsilon}_6$	2.5 m/s	24.490	10	

of fracture stress and strain by Brokmann *et al.*[23] and Berlinger *et al.*[31]. The CDF of the 2PW is given by:

$$P(\varepsilon)=1-\exp[(-\frac{\varepsilon}{\eta})^{\beta}] \quad (1)$$

with the scale parameter η and the shape parameter β[32]. The notation $\exp(x)=e^x$ is used in the context of this work to improve readability. The scale parameter η is the expected value for the strain at which $1-e^{-1}\approx63.2\%$ of all the specimens have already failed during the experimental procedure and, hence, is a physically relevant parameter. The shape parameter β is an indicator of dispersion in the fracture strain population; generally, large values for β yield narrower distributions, whereas small values yield broader distributions. However, it should be highlighted that β is only an indicator and not an independent measure of dispersion, as the parameter is dependent on η if the distribution is shifted in ε[33]. We also want to mention that the use of the 2PW is suitable for this field of application because, in contrast to other common distribution functions such as the normal distribution, the 2PW is also able to capture skewed or asymmetric data probability densities.

The basis for statistical analysis is a set of experimentally measured fracture strains that do not contain information on their probability of occurrence. The single fracture strains ε_i, $i \in \{1,2,...,N\}$, in the set of size N are an outcome of variate ε. Thus, ε_i is the quantile assigned to the probability p_i of the unknown CDF $P(\varepsilon)$. To estimate the parameters β and η of the CDF, first, the fracture strain sample is sorted in ascending order as $\varepsilon_1<\varepsilon_2<\cdots<\varepsilon_N$. The occurrence probability for a new observation ε_{N+1} being less than or equal to ε_i is $P(\varepsilon_{N+1}\leq\varepsilon_i)=p_i$. To define the sample quantiles $\varepsilon_i=\mathrm{P}^{-1}(p_i)$, Weibull's formula for the plotting positions is used, which assigns each ε_i to

$$p_i=\frac{i}{N+1}, \quad (2)$$

depending on position i in the order. The combination of the sample quantile and plotting position yields the coordinate points $(\varepsilon_i|p_i)$. Although many possible formulas for defining sample quantiles can be found in the relevant literature, the one by Weibull is chosen within the course of this study because it is sufficient for use with PMMA fracture strains[31,33,34].

In practice, the 2PW is often fitted to the coordinate points by linear regression after transforming the coordinate system, yielding the Weibull probability plot[35]. However, as the coordinate transformation brings an unwanted weighting of the residual into the fit[36], the given 2PW CDF function parameters are determined by minimizing the residual sum of squares (RSS):

$$RSS=\Sigma_{i=1}^{N}[p_i-P(\varepsilon_i)]^2. \quad (3)$$

2. Goodness of fit

To investigate the quality of an achieved CDF fit, the Generalized Anderson-Darling (GAD) test, which can account for the use of different definitions for the plotting positions, is used[34]. The test statistic A_{G}^2 for the GAD test is given as

$$A_{\mathrm{G}}^2=N\{-1-\ln[\mathrm{P}(\varepsilon_N)(1-P(\varepsilon_i))]+\Sigma_{i=1}^{N-1}[p_i^2\ln(\frac{P(\varepsilon_{i+1})}{P(\varepsilon_i)})-(p_i-1)^2\ln(\frac{(1-P(\varepsilon_{i+1})}{1-P(\varepsilon_i)})]\}. \quad (4)$$

This test statistic is a measure of the deviation of the CDF from the coordinate points of the sample in which the function tails are weighted higher. To make a general statement on the statistical significance of the received test statistic, Table 2 is provided. Analogous to the procedure proposed by Ref. 34, the GAD test statistics are determined for commonly examined significance levels α. Thus, the calculated A_{G}^2 from Eq. (4) is rated by comparison with the listed thresholds.

A significance level of α=5% is usually considered as the limit for evaluation. If the test statistic A_{G}^2 is rated with a higher significance, the fitted CDF is assumed to match the experimental data.

3. Cramér-von Mises test

Within the course of this study, the two-sample CvM test[37] is used to investigate whether the two samples of fracture strains obtained at different strain rates may come from the same unknown CDF. The CvM test statistic T is calculated as follows:

$$T=\frac{NM}{(N+M)^2}(\Sigma_{i=1}^{N}[F_N(x_i)-G_M(x_i)]^2+\Sigma_{i=1}^{M}[F_N(y_j)-G_M(y_j)]^2) \quad (5)$$

with the two samples $x_1,x_2,\ldots,x_N$ and $y_1,y_2, \ldots, y_N$ and their corresponding empirical distribution functions F_N and G_M (with sample sizes N and M, respectively). Here, the variance of T is

$$\mathrm{Var}(T)=\frac{1}{45}\frac{M+N+1}{(M+N)^2}\frac{4MN(M+N)-3(M^2+N^2)-2MN}{4MN}. \quad (6)$$

By comparing

$$T_{\mathrm{mod}}=[\frac{T\frac{1}{6}\frac{1}{6(M+N)}}{45\,\mathrm{Var}(T)}]+\frac{1}{6} \quad (7)$$

with the critical threshold T_α of the limiting distribution, the significance of the observed value for T_{mod} can be determined. The null hypothesis of CvM that the two samples stem from the same distribution is rejected if the critical value T_α is exceeded by T_{mod}. Some selected critical values T_α are listed in Table 3[38].

4. Coefficient of determination

To estimate the goodness of the later proposed statistical model, the coefficient of determination[39]

$$R^2=1-\frac{\Sigma[p_i-P(\varepsilon_i)]^2}{\Sigma[p_i-\tilde{p}]^2} \quad (8)$$

is used. This provides a measure of how well the coordinate points of the sample reproduce the fitted CDF. The values for the coefficient of determination range from $0\leq R^2\leq 1$, where a value of 0 indicates no correlation and a value of 1 indicates a perfect fit between the model and empirical data.

RESULTS

Fracture strain distributions

The obtained strain-rate dependent CDFs are displayed in Fig. 1. As can be observed, the coordinate points of the respective samples are neatly captured by the 2PW CDFs. In Table 4, the determined function parameters η and β as well as the corresponding RSS and A_G^2 values are listed for each strain rate. The results imply that the scale parameter η decreases, whereas the shape parameter β increases with the strain rate.

Furthermore, the distributions at high strain rates seem to correlate strongly with each other despite a strong increase in the strain rate between the samples. This indicates that a limiting distribution is formed at high strain rates. To statistically corroborate this observation, CvM is used for pairwise comparison. The T values obtained from the calculations are listed in Table 5. A significance level α of 0.01 is chosen to test the null hypothesis H_0 stating that the two samples being

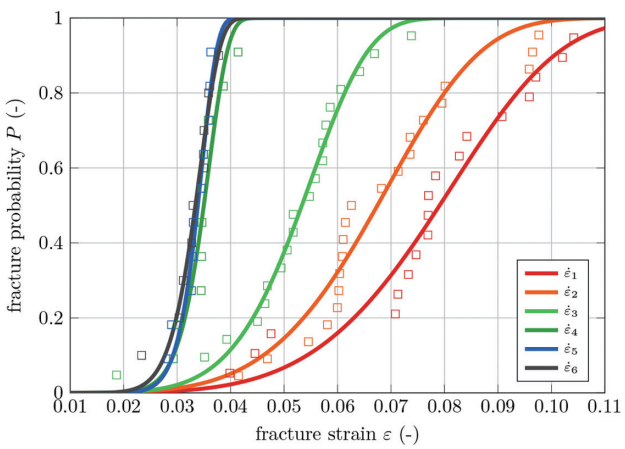

Fig. 1 Strain-rate dependent CDFs of the observed fracture strains.

Table 2 Limits of the GAD test at different significance levels α

sample size N	Percentage level (%)				
	15	10	5	2.5	1
5	0.562	0.607	0.682	0.756	0.859
10	0.600	0.662	0.774	0.892	1.057
15	0.606	0.676	0.801	0.935	1.127
20	0.606	0.680	0.812	0.954	1.158

Table 3 Critical thresholds of T_α of the CvM[38]

	Significance level α			
	0.05	0.10	0.25	0.50
T_α	0.461	0.347	0.209	0.119

Table 4 2PW CDF function parameters and corresponding goodness of fit

Ref.	Strain rate (1/s)	η	β	*RSS*	A_G^2
$\dot{\varepsilon}_1$	6.920×10^{-4}	0.0851	5.003	0.0676	0.512
$\dot{\varepsilon}_2$	6.920×10^{-3}	0.0726	4.945	0.0803	1.164
$\dot{\varepsilon}_3$	6.920×10^{-2}	0.0567	6.024	0.0210	0.496
$\dot{\varepsilon}_4$	4.898	0.0362	10.614	0.0797	0.826
$\dot{\varepsilon}_5$	9.796	0.0348	12.775	0.0351	0.455
$\dot{\varepsilon}_6$	24.490	0.0347	10.061	0.0182	0.282

Table 5 Results of the pairwise CvM comparison between strain rates

Sample 1	Sample 2	T_{mod}	$T_{crit,\alpha=0.05}$	H_0
$\dot{\varepsilon}_4$	$\dot{\varepsilon}_5$	0.0950	0.461	true
$\dot{\varepsilon}_5$	$\dot{\varepsilon}_6$	0.0350	0.461	true
$\dot{\varepsilon}_4$	$\dot{\varepsilon}_6$	0.0817	0.461	true

compared here are an outcome of the same distribution. Concerning Table 5, the null hypothesis can be considered true, with a probability of 99 % for each case. Therefore, we postulate that a lower limit of fracture strain distributions is reached at high strain rates with a minimum scale parameter η_{dyn} and maximum shape parameter β_{dyn}.

Rate-dependency of the 2PW parameters

In addition to the distribution limit present at high strain rates, it is assumed that the quasi-static distribution can also be considered a limiting case, as it can be presumed for quasi-static loading that a further reduction in strain rate will no longer cause a change in the distribution of fracture strains. Thus, it can be stated that there also exists a physically reasonable limiting case of maximum dispersion (*i.e.*, a minimal β) and a maximum scale parameter η. For scale parameter η, this behavior can be described phenomenologically, using an exponential equation:

$$\eta(\dot{\varepsilon},\gamma_1,\gamma_2)=[\eta_{qs}-\eta_{dyn}]\exp(\gamma_1\dot{\varepsilon}^{\gamma_2})+\eta_{dyn}, \quad (9)$$

where η_{qs} is the experimentally obtained maximum quasi-static scale parameter, η_{dyn} is the experimental mean scale parameter that is achieved at high rates, and γ_1 and γ_2 are the fit parameters. It has already been established that there exists a limiting minimum β_{qs} for the quasi-static case, but since the value for β is dependent on $\eta(\dot{\varepsilon})$ resulting from a shift of the CDF with increasing $\dot{\varepsilon}$, we assume that the function

$$\beta(\eta(\dot{\varepsilon},\gamma_1,\gamma_2),\gamma_3,\gamma_4)=\gamma_3\exp(\gamma_4\eta(\dot{\varepsilon},\gamma_1,\gamma_2))+\beta_{qs} \quad (10)$$

with the two fit parameters γ_3 and γ_4 for modeling, which is implicitly dependent on the strain rate. The selected fit function is carefully chosen such that the dependency of β on the strain rate possesses the observed limiting minimum β_{qs} (which is obtained experimentally from the quasi-static test) and maximum β_{dyn}, which will result from the fit.

To obtain the parameters γ_1 of the proposed model, the $\eta(\dot{\varepsilon},\gamma_1,\gamma_2)$ functions are fitted to the obtained parameters given in Table 4 through the *RSS*, yielding parameters γ_1 and γ_2 (*cf.* the progression shown in Fig. 2). As the rate-dependency is strongest between smaller strain rates, a weighting function $\psi(i)=1/i$ is multiplied by the squared residuals in Eq. (3) to assign weights to the parameters attained in the lower function areas. Then, $\beta(\eta(\dot{\varepsilon}))$ is fitted to $\eta(\dot{\varepsilon})$, yielding γ_3 and γ_4. For a better overview, this relationship is illustrated in Fig. 3. The values of the fit parameters determined from this procedure are listed in Table 6.

The curves of η and β over the strain rate resulting from the proposed model are displayed in Fig. 2, with the experimentally obtained values for the scale and shape parameters at each tested strain rate. It can be observed that the rate-dependencies of both the scale and shape parameters are captured by the model function with good agreement.

To validate the model generated following this procedure, the CDFs from Fig. 1 are recreated with parameters following the model functions at the given strain rates. The modelled CDFs and original coordinate points are displayed in Fig. 4. It can be observed visually that the recreated CDFs correspond to the coordinate points with good agreement, which indicates that the proposed model for the description of rate-dependency for the form and shape parameters is reasonably accurate. The coefficients of determination between the plotting positions and respective recreated CDFs are listed in Table 7. The mean coefficient of determination of 90.3%

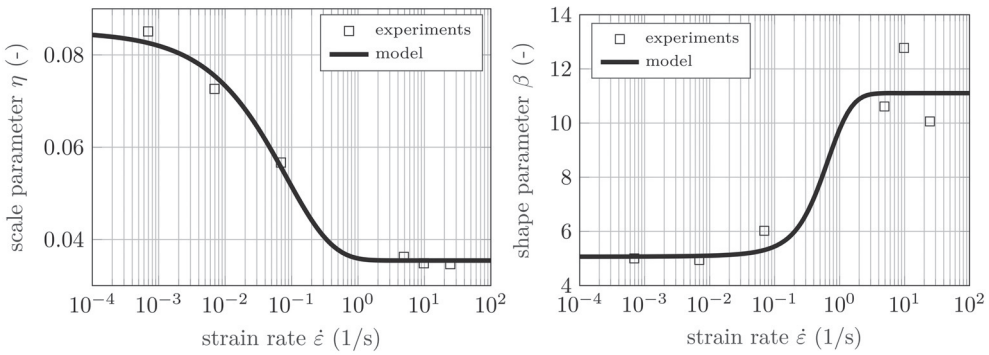

Fig. 2 Modelled rate-dependency of the 2PW parameters η and β.

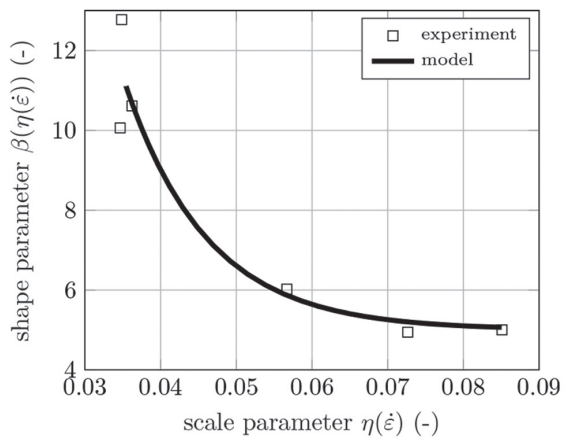

Fig. 3 Fitted relationship between $\beta(\eta(\dot{\varepsilon}))$ and $\eta(\dot{\varepsilon})$.

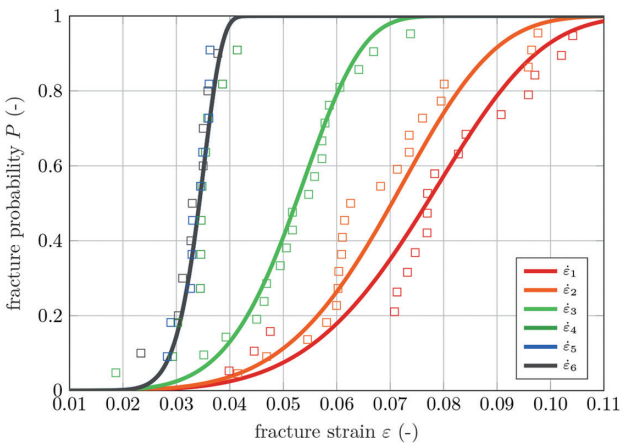

Fig. 4 Strain-rate dependent CDFs obtained from the proposed model.

Table 6 Fitted parameters γ_i of the model functions

γ_1	γ_2	γ_3	γ_4
−4.701	0.620	158.587	−91.930

Table 7 Correlation coefficients between measurements and modelled CDFs

Ref.	Strain rate (1/s)	R^2
$\dot{\varepsilon}_1$	6.920×10^{-4}	0.927
$\dot{\varepsilon}_2$	6.920×10^{-3}	0.910
$\dot{\varepsilon}_3$	6.920×10^{-2}	0.974
$\dot{\varepsilon}_4$	4.898	0.821
$\dot{\varepsilon}_5$	9.796	0.900
$\dot{\varepsilon}_6$	24.490	0.887
	Mean:	0.903

also suggests that the model is in good agreement with the original coordinate points. By gathering more distribution functions at further strain rates between quasi-static and dynamic loading, the tuning of the rate-dependency model could be improved, leading to smaller deviations between the model and original CDFs and a better fit on the coordinate points of the samples.

Fracture probability depending on strain and strain rate

By making the parameters η and β of the 2PW dependent on the strain rate, a function for the failure probability is obtained, which is explicitly dependent on the strain and implicitly dependent on the strain rate *via* the modelled rate-dependence of $\eta(\dot{\varepsilon})$ and $\beta(\eta(\dot{\varepsilon}))$, yielding:

$$P(\varepsilon,\dot{\varepsilon})=1-\exp[(-\frac{\varepsilon}{\eta(\dot{\varepsilon})})^{\beta(\eta(\dot{\varepsilon}))}] \quad (11)$$

(*cf.* Eq. (1)). The resulting models for $P(\varepsilon,\dot{\varepsilon})$ are shown in Fig. 5.

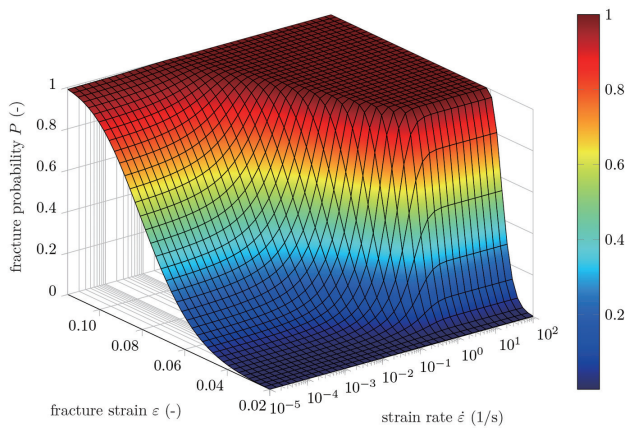

Fig. 5 Relationship between fracture strain, strain rate and occurrence probability obtained from the proposed model.

DISCUSSION

The obtained model of $P(\varepsilon,\dot{\varepsilon})$ now allows the determination of the fracture probability of a component consisting of the investigated material at a given strain and strain rate. We shall highlight two special use cases for application of the model.

To begin with, we suppose that this model can be used in a scientific context, *e.g.*, in stochastic finite element simulations. The approach for this use case is shown in Fig. 6; where, hypothetically, a random number generator could first be used to calculate a random occurrence probability, which is then used to obtain tabulated values of the fracture strain according to this probability, depending on the strain rate. These tabulated values can then be used as failure criteria for finite element simulations of various components under different boundary conditions. By checking on whether the simulation will result in a component failure, one obtains the probability of the component failing after multiple repetitions of the simulations. This approach could be used to conduct an increasing number of numerical studies, saving expensive and time-consuming component tests, which could be of particular benefit in the development of biomedical components. Thus, an increased number of simple material tests could reduce the need for a large number of component tests, as is seen commonly in the case of crash simulations in the automotive sector.

A second application could be designing a component with a statistical safety target (*cf.* Fig. 7), which we suppose could be of great use in a clinical context, *e.g.*,

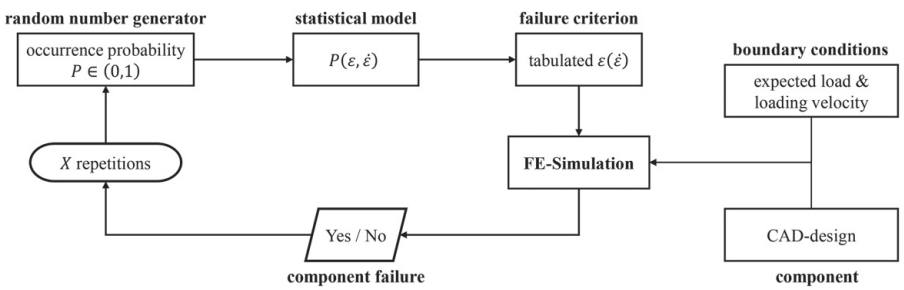

Fig. 6 Implementation of the proposed model in stochastic finite element simulations.

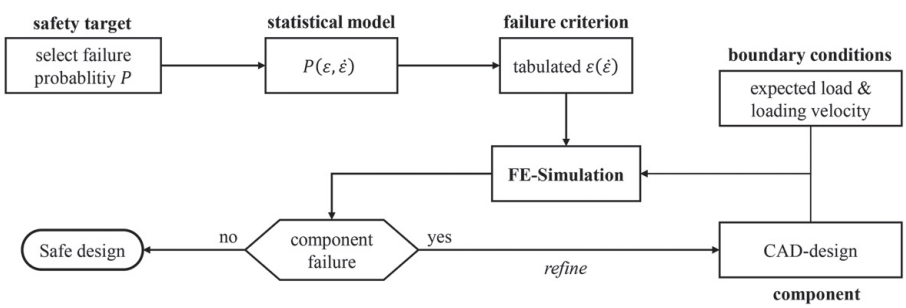

Fig. 7 Clinical implementation of the proposed model.

when designing fixed partial dentures or other dental restorations. In this use case, the practitioner must first select the accepted failure probability of a component. This target can then be used to select a failure criterion of fracture strains at different strain rates from the proposed $P(\varepsilon,\dot{\varepsilon})$ model, similar to the previously described application. By simulating the desired component (akin to Schrader *et al.*[17]) at the expected boundary conditions (*i.e.*, chewing velocity and chewing force in the case of a dental restoration), one obtains an indication of whether the planned supply can withstand the expected load . If the simulated component happens to fracture, the restoration must be redesigned; otherwise, the planned restoration can be manufactured. This could be of potential use, especially in digital dentistry, as CAD models obtained from intraoral scans could be directly simulated with the desired safety target by the intraoral scanner software with expected chewing forces and velocities as estimated by the dentist, depending on the individual needs of the patient. Until now, in daily dental practice, the experience of the dentist or dental technician has often been relied upon in addition to the study results. With the presented methodology, the critical points in the design of a prosthesis can be recognized early. This, in effect, allows a patient's individual design to ultimately improve patient safety, well-being, and the aesthetics of the resulting dental restoration.

In our study, we relied heavily on the results obtained by Schmidt *et al.*[24]. The data of Schmidt *et al.*[24] was considered suitable for statistical evaluation in the course of this work as, to the authors knowledge, it is the only study to investigate the rate-dependent behavior of a commercial dental PMMA and provided a sufficiently large database to calibrate a statistical model. Furthermore, loading in 3PBT achieves uniaxial tension, which is the most critical load case for polymeric materials. The used material Telio CAD is cross-linked PMMA with a percentage by weight of 99.5%, to which pigments (less than 1% by weight) have been added[7,9,10]. The use of industrially produced and standardized blanks allowed a high degree of material homogeneity[40-42]. Furthermore, we considered it important to rely on a material that has been clinically approved and examined in numerous other studies (see, Refs. 7, 8, 10, 11).

It should also be noted that an additional experimental validation of the proposed model could be advantageous, especially in other loading rates than the ones to which the model was calibrated. Unfortunately, this could not be performed in this study due to lack of funding. However, considering the comparatively large underlying data base and the amount of sampling steps of the tested strain rates from Schmidt *et al.*[24], it is believed that the model allows interpolation of the strain rate dependent behavior without a significant loss of accuracy.

We suppose that the proposed model can be directly applied to other polymer-based materials such as other thermoplastics or hybrid materials, as these generally show rate-dependent, stochastic fracture behavior to different extents. Because of the pragmatic phenomenological approach, models can be easily developed from a database of material tests at different strain rates by fitting the four parameters γ_1, γ_2, γ_3, and γ_4 to the obtained fracture statistics, which can then be implemented in different applications. Owing to different findings on the rate-dependency of the 2PW parameters η and β and careful selection of model functions in this study, an extrapolation of the model is also possible, allowing its use in many different applications.

However, there are still opportunities to expand the proposed failure model in future studies. For example, stress triaxiality cannot be considered in a database. Uniaxial tension, as obtained in 3PBT, is the most critical load case because polymers can bear higher loads in shear than in tension. However, a more detailed analysis characterizing the shear properties could provide valuable insights into the fracture behavior and improve the simulation results. Hence, we suggest to also study the influence of the stress profiles obtained with different loading geometries (*e.g.*, 3PB, 2PB, pure bending and pure tension) in the fracture behavior. Furthermore, given the data of Schmidt *et al.*[24], the influences of humidity and temperature were not investigated, which is of interest *in vivo*. Hence, incorporating the effects of temperature and humidity into the proposed stochastic model may also be an interesting topic for future studies. In the context of prostheses, it would certainly be of interest to consider fatigue behavior, *e.g.*, by investigating the fracture strain at different numbers of load cycles. However, for all these studies, a very large database is necessary, as the parameters η and β would have to be determined for different conditions of the mentioned variables and related to these quantities by different (phenomenological) relationships. If such relationships are found, we assume that they can be integrated into the model of fracture probability according to Eq. (11).

The novel methodology presented makes it possible to predict the possible survival probability of a polymeric component in advance. This allows clinicians or researchers to clearly define in advance the kind of material that is suitable for clinical application. With the presented methodology, the critical points in the design of biomedical components can be recognized early. For example, considering the ever-increasing digitalization of dentistry, the implementation of intraoral scanners (IOS) or computer-aided design/computer-aided manufacturing (CAD/CAM) programs to produce patient-specific treatments is also deemed possible. This would allow the IOS software to suggest a possible material selection directly after the scan and not define critical areas based on the minimum layer thicknesses alone, as is the case today. Furthermore, framework conditions can be created when planning future material examinations to sensibly determine which examination series should be carried out. Survival probabilities or thermal cycling are also conceivable because material characterization can also be carried out in advance with materials that have already been thermally pretreated. These results are later incorporated into the statistical analysis. Given

the wide and almost unmanageable choice of materials, a possible calculation of failure probability in advance is both appropriate and necessary.

CONCLUSIONS

The results of this study show a prominent rate-dependent and stochastic fracture behavior of the investigated dental PMMA. Therefore, it is assumed that the investigation of both the rate-dependent and stochastic fracture behavior of dental biomaterials offers great potential for improving the structural safety of prostheses. This, in effect, may assist decreasing health risks for the patient if considered during a prosthesis' design stage. Within the limitations of this study, the following conclusions are drawn.

- The rate-dependency of PMMA's fracture strains was significant and must not be neglected in dental biomaterials science. A lower limit of fracture strain was reached at high strain rates.
- It is assumed that the proposed methodology for determining the structural safety of dental biomaterials under different loading conditions can likely be transferred to materials other than PMMA. A future application of the methodology to other biomaterials such as hybrid ceramics or resin composites is deemed worthwhile.
- The statistical investigation of a material in advance can save time and cost-intensive preliminary test series, which made material examinations more effective.

ACKNOWLEDGMENTS

The study was co-funded by the Flexi Funds of the Research Campus of Central Hessen, Germany.

CONFLICTS OF INTEREST

The authors declare no conflicts of interest.

REFERENCES

1) Frazer RQ, Byron RT, Osborne PB, West KP. PMMA: An essential material in medicine and dentistry. J Long Term Eff Med Implants 2005; 15: 629-639.
2) Richeton J, Ahzi S, Vecchio KS, Jiang FC, Adharapurapu RR. Influence of temperature and strain rate on the mechanical behavior of three amorphous polymers: Characterization and modeling of the compressive yield stress. Int J Solids Struct 2006; 43: 2318-2335.
3) Vallo CI. Flexural strength distribution of a PMMA-based bone cement. J Biomed Mater Res 2002; 63: 226-236.
4) Vallo CI. Influence of load type on flexural strength of a bone cement based on PMMA. Polym Test 2002; 21: 793-800.
5) Kraft J. Polymethylmethacrylate —A review. J Foot Surg 1977; 16: 66-68.
6) Lloyd AW, Faragher RG, Denyer SP. Ocular biomaterials and implants. Biomaterials 2001; 22: 769-785.
7) Güth J-F, Zuch T, Zwinge S, Engels J, Stimmelmayr M, Edelhoff D. Optical properties of manually and CAD/CAM-fabricated polymers. Dent Mater J 2013; 32: 865-871.
8) Kelvin Khng KY, Ettinger RL, Armstrong SR, Lindquist T, Gratton DG, Qian F. In vitro evaluation of the marginal integrity of CAD/CAM interim crowns. J Prosthet Dent 2016; 115: 617-623.
9) Rosentritt M, Raab P, Hahnel S, Stöckle M, Preis V. In-vitro performance of CAD/CAM-fabricated implant-supported temporary crowns. Clin Oral Investig 2017; 21: 2581-2587.
10) Wiegand A, Stucki L, Hoffmann R, Attin T, Stawarczyk B. Repairability of CAD/CAM high-density PMMA- and composite-based polymers. Clin Oral Investig 2015; 19: 2007-2013.
11) Yao J, Li J, Wang Y, Huang H. Comparison of the flexural strength and marginal accuracy of traditional and CAD/CAM interim materials before and after thermal cycling. J Prosthet Dent 2014; 112: 649-657.
12) Herráez-Galindo C, Rizo-Gorrita M, Maza-Solano S, Serrera-Figallo M-A, Torres-Lagares D. A review on CAD/CAM yttria-stabilized tetragonal zirconia polycrystal (Y-TZP) and polymethyl methacrylate (PMMA) and their biological behavior. Polymers (Basel) 2022; 14: 906.
13) Ionescu RN, Totan AR, Imre MM, Țâncu AMC, Pantea M, Butucescu M, *et al.* Prosthetic materials used for implant-supported restorations and their biochemical oral interactions: A narrative review. Materials (Basel) 2022; 15: 1016.
14) Gu Y, Bai Y, Xie X. Bite force transducers and measurement devices. Front Bioeng Biotechnol 2021; 9: 665081.
15) Larson TD. The effect of occlusal forces on restorations. Northwest Dent 2012; 91: 25-7, 29-35.
16) Hou R, Zhou H, Hu K, Ding Y, Yang X, Xu G, *et al.* Thorough documentation of the accidental aspiration and ingestion of foreign objects during dental procedure is necessary: Review and analysis of 617 cases. Head Face Med 2016; 12 : 23.
17) Schrader P, Kolling S, Schlenz MA, Wöstmann B, Schmidt A. Finite element simulation of fixed dental prostheses made from PMMA —Part II: Material modeling and nonlinear finite element analysis. Dent Mater J 2021; 40: 894-902.
18) Iacono F, Pirani C, Arias A, de la Macorra JC, Generali L, Gandolfi MG, *et al.* Impact of a modified motion on the fatigue life of NiTi reciprocating instruments: A Weibull analysis. Clin Oral Investig 2019; 23: 3095-3102.
19) Yamaguchi S, Kani R, Kawakami K, Tsuji M, Inoue S, Lee C, *et al.* Fatigue behavior and crack initiation of CAD/CAM resin composite molar crowns. Dent Mater 2018; 34: 1578-1584.
20) Gonçalves TMSV, Teixeira KN, de Oliveira JMD, Gama LT, Bortolini S, Philippi AG. Surface treatments to improve the repair of acrylic and bis-acryl provisional materials. Am J Dent 2018; 31: 199-204.
21) Quinn JB, Quinn GD. A practical and systematic review of Weibull statistics for reporting strengths of dental materials. Dent Mater 2010; 26: 135-147.
22) Zucuni CP, Guilardi LF, Rippe MP, Pereira GKR, Valandro LF. Polishing of ground Y-TZP ceramic is mandatory for improving the mechanical behavior. Braz Dent J 2018; 29: 483-491.
23) Brokmann C, Berlinger M, Schrader P, Kolling S. Fraktographische Bruchspannungs —Analyse von Acrylglas. ce/papers 2019; 3: 225-237.
24) Schmidt A, Schrader P, Schlenz MA, Wöstmann B, Kolling S. Is the assumption of linear elasticity within prosthodontics valid for polymers? —An exemplary study of possible problems. Dent Mater J 2021; 40: 52-60.
25) Mulliken AD, Boyce MC. Mechanics of the rate-dependent elastic–plastic deformation of glassy polymers from low to high strain rates. Int J Solids Struct 2006; 43: 1331-1356.
26) Wu H, Ma G, Xia Y. Experimental study of tensile properties of PMMA at intermediate strain rate. Mater Lett 2004; 58: 3681-3685.
27) Fleck NA, Stronge WJ, Liu JH. High strain-rate shear response of polycarbonate and polymethyl methacrylate. Proc

R Soc Lond A 1990; 429: 459-479.
28) Bauwens-Crowet C. The compression yield behaviour of polymethyl methacrylate over a wide range of temperatures and strain-rates. J Mater Sci 1973; 8: 968-979.
29) Bauwens-Crowet C, Bauwens JC, Homès G. Tensile yield-stress behavior of glassy polymers. J Polym Sci A Polym Phys 1969; 7: 735-742.
30) Schmidt A, Kididane I, Schlenz MA, Wöstmann B, Kolling S, Schrader P. Finite element simulation of fixed dental prostheses made from PMMA —Part I: Experimental investigation under quasi-static loading and chewing velocities. Dent Mater J 2021; 40: 704-711.
31) Berlinger M, Schrader P, Kolling S. Analyses on the strain-rate dependent fracture behaviour of PMMA for stochastic simulations. 15. LS-Dyna Forum, Bamberg. 2018. Available at: https://www.dynamore.de/de/download/papers/2018-ls-dyna-forum/papers-2018/dienstag-16.-oktober/crash-materials-failure.
32) Ballarini R, Pisano G, Royer-Carfagni G. The lower bound for glass strength and its interpretation with generalized Weibull statistics for structural applications. J Eng Mech 2016; 142: 4016100.
33) Berlinger M. A Methodology to Model the Statistical Fracture Behavior of Acrylic Glasses for Stochastic Simulation. 1st ed. 2021. Wiesbaden: Springer Fachmedien Wiesbaden; Imprint Springer Vieweg; 2021. Springer eBook Collection; 59.
34) Berlinger M, Kolling S, Schneider J. A generalized Anderson-Darling test for the goodness-of-fit evaluation of the fracture strain distribution of acrylic glass. Glass Struct Eng 2021; 6: 195-208.
35) Lai C-D. Generalized Weibull Distributions. Berlin, Heidelberg: Springer Berlin Heidelberg; 2014.
36) Makkonen L. Plotting positions in extreme value analysis. J Appl Meteor Climatol 2006; 45: 334-340.
37) Anderson TW. On the distribution of the two-sample Cramer-von Mises criterion. Ann Math Statist 1962; 33: 1148-1159.
38) Anderson TW, Darling DA. Asymptotic theory of certain "Goodness of Fit" criteria based on stochastic processes. Ann Math Statist 1952; 23: 193-212.
39) Kvålseth TO. Note on the R2 measure of goodness of fit for nonlinear models. Bull Psychon Soc 1983; 21: 79-80.
40) Almohareb T, Alkatheeri MS, Vohra F, Alrahlah A. Influence of experimental staining on the color stability of indirect computer-aided design/computer-aided manufacturing dental provisional materials. Eur J Dent 2018; 12: 269-274.
41) Elagra MI, Rayyan MR, Alhomaidhi MM, Alanaziy AA, Alnefaie MO. Color stability and marginal integrity of interim crowns: An in vitro study. Eur J Dent 2017; 11: 330-334.
42) Rayyan MM, Aboushelib M, Sayed NM, Ibrahim A, Jimbo R. Comparison of interim restorations fabricated by CAD/CAM with those fabricated manually. J Prosthet Dent 2015; 114: 414-419.